

Discrete clouds of neutral gas between the galaxies M31 and M33

Spencer A. Wolfe¹, D. J. Pisano¹, Felix J. Lockman², Stacy S. McGaugh³ & Edward J. Shaya⁴

Spiral galaxies must acquire gas to maintain their observed level of star formation beyond the next few billion years¹. A source of this material may be the gas that resides between galaxies, but our understanding of the state and distribution of this gas is incomplete². Radio observations³ of the Local Group of galaxies have revealed hydrogen gas extending from the disk of the galaxy M31 at least halfway to M33. This feature has been interpreted to be the neutral component of a condensing intergalactic filament⁴, which would be able to fuel star formation in M31 and M33, but simulations suggest that such a feature could also result from an interaction between both galaxies within the past few billion years (ref. 5). Here we report radio observations showing that about 50 per cent of this gas is composed of clouds, with the rest distributed in an extended, diffuse component. The clouds have velocities comparable to those of M31 and M33, and have properties suggesting that they are unrelated to other Local Group objects. We conclude that the clouds are likely to be transient condensations of gas embedded in an intergalactic filament and are therefore a potential source of fuel for future star formation in M31 and M33.

A recent study⁶ of the region between M31 and M33 using the Robert C. Byrd Green Bank Telescope (GBT) at 9' angular resolution has confirmed the presence of neutral hydrogen at levels of a few times 10^{17} cm^{-2} . The study also showed that this neutral gas has a velocity similar to the systemic velocities of M31 and M33, and is thus not the product of confusion with foreground emission from the Milky Way. The sensitivities of the observations were, however, insufficient to provide a detailed understanding of the structure and extent of this gas. Observations were needed with high angular resolution, high velocity resolution and high sensitivity to distinguish clouds from diffuse gas, and an intergalactic filament from tidal debris. Determining the origin of the gas is important, for if it is from an intergalactic filament, it would represent a new source of material to fuel future star formation in M31 and M33.

We have mapped a portion of the hydrogen gas feature between M31 and M33 with improved sensitivity and higher angular and velocity resolution using the GBT. We detect seven clouds (Fig. 1); Table 1 lists their properties. The positions and velocities of the brightest clouds are consistent with previous GBT results⁶. The primary difference between

the results from the Westerbork Synthesis Radio Telescope (WSRT) survey³, which used that array as a collection of single dishes, and our high-resolution data is that here the H I emission is resolved into features approximately the size of a GBT beamwidth or smaller, and at much higher column densities. The GBT data convolved to 49' angular resolution reproduce the same basic morphology as the WSRT data. The total H I mass detected is $(1.2 \pm 0.1) \times 10^6 M_{\odot}$ above a level of $3.0 \times 10^{17} \text{ cm}^{-2}$, $(1.3 \pm 0.1) \times 10^6 M_{\odot}$ above $1.0 \times 10^{17} \text{ cm}^{-2}$ and $(1.9 \pm 0.1) \times 10^6 M_{\odot}$ above $1.0 \times 10^{16} \text{ cm}^{-2}$ (here M_{\odot} is the solar mass). These values do not appear to be consistent with the relationship between the mass of neutral atomic hydrogen (M_{HI}) and its column density (N_{HI}) predicted by simulations of intergalactic H I at low redshift⁷. The total H I mass measured across the entire map is $(2.6 \pm 0.2) \times 10^6 M_{\odot}$, identical to the total H I mass from the WSRT data over the same area. There is probably additional mass present in the form of ionized gas, as at such low column densities photoionization of the H I by the extragalactic radiation field becomes significant⁸.

About 50% of the neutral hydrogen is in clouds, whose diameters range from ≤ 2.4 kpc to 6.4 kpc. This is the size range of dwarf galaxies; however, although stellar surveys^{9,10} have detected dwarf galaxies around M31 as well as potential dwarf galaxy remnants, there are no reports of stellar over-densities at the positions of these clouds¹⁰, even though there is no lack of stellar streams in the general vicinity¹¹. The clouds lie much farther from M31 and M33 than each galaxy's respective high-velocity cloud (HVC) population and also lie closer to the systemic velocities of M31 and M33 than the HVCs (Fig. 2). The clouds are also kinematically cooler as a population than the HVCs, with a lower inter-cloud velocity dispersion by a factor of two to five.

We estimate the baryonic mass and circular rotation speed about the cloud centre for the clouds as well as for the HVCs and dwarf galaxies of M31 and M33, and plot them with the baryonic Tully–Fisher relation^{12,13} (Fig. 3). This allows us to compare the clouds to other members of the Local Group. The clouds are offset from the Tully–Fisher relation for rotating disk galaxies; they occupy a similar region in the Tully–Fisher plane as the HVCs and dwarfs, but cluster more tightly.

If the linewidths of the clouds are interpreted as an equilibrium velocity representative of the gravitational potential, then the clouds would be highly dark-matter dominated. The virial mass of every cloud

Table 1 | H I cloud properties

Cloud ...	RA (h min s)	Dec. (° ' ")	LSR velocity (km s^{-1})	FWHM (km s^{-1})	$T_{\text{B,Peak}}$ (mK)	$\log[N_{\text{HI,Peak}} (\text{cm}^{-2})]$	M_{HI} (M_{\odot})	Diameter (kpc)
1	01 24 42	+37 23 02	-297 ± 1	23 ± 3	47 ± 4	17.6 ± 0.04	$(1.2 \pm 0.2) \times 10^5$	$\leq 2.8 \pm 1$
2	01 20 52	+37 16 58	-236 ± 1	28 ± 2	69 ± 4	17.8 ± 0.03	$(3.5 \pm 0.3) \times 10^5$	6.4 ± 1
3	01 19 25	+37 31 12	-226 ± 2	28 ± 4	41 ± 4	17.6 ± 0.04	$(1.1 \pm 0.2) \times 10^5$	$\leq 2.4 \pm 1$
4	01 08 30	+37 44 51	-277 ± 1	34 ± 3	91 ± 4	17.9 ± 0.02	$(4.0 \pm 0.3) \times 10^5$	4.8 ± 1
5	01 05 09	+36 23 28	-209 ± 4	26 ± 3	34 ± 4	17.5 ± 0.05	$(4.2 \pm 1.0) \times 10^4$	$\leq 2.4 \pm 1$
6	01 03 10	+36 01 46	-282 ± 4	29 ± 3	39 ± 4	17.6 ± 0.05	$(1.4 \pm 0.2) \times 10^5$	$\leq 3.2 \pm 1$
7	01 17 02	+36 49 34	-309 ± 2	24 ± 4	10 ± 2	17.0 ± 0.1	$(4.0 \pm 1.0) \times 10^4$	$\leq 3.4 \pm 1$

RA and Dec. are respectively the right ascension and declination of each cloud; LSR, Local Standard of Rest; FWHM, full-width at half-maximum of the H I line; $T_{\text{B,Peak}}$, peak brightness temperature; $N_{\text{HI,Peak}} = 1.82 \times 10^{18} T_{\text{B,Peak}} \Delta v$ is the peak column density, where $\Delta v \approx 5 \text{ km s}^{-1}$; M_{HI} is the H I mass of the cloud, in solar masses, measured to the 3σ column density contour in the maps; diameter is measured to the same contour along the major axis of the cloud, if one is apparent. The ± 1 kpc error in the diameter is due to the pixel size in our maps projected to a distance of ~ 800 kpc. The values for cloud 7 were obtained from the 15' map. Quantities were calculated assuming a distance to the clouds of 800 kpc (ref. 6).

¹Department of Physics, West Virginia University, PO Box 6315, Morgantown, West Virginia 26506, USA. ²National Radio Astronomy Observatory, PO Box 2, Green Bank, West Virginia 24944, USA.

³Department of Astronomy, Case Western Reserve University, Cleveland, Ohio 44106, USA. ⁴Department of Astronomy, University of Maryland, College Park, Maryland 20742, USA.

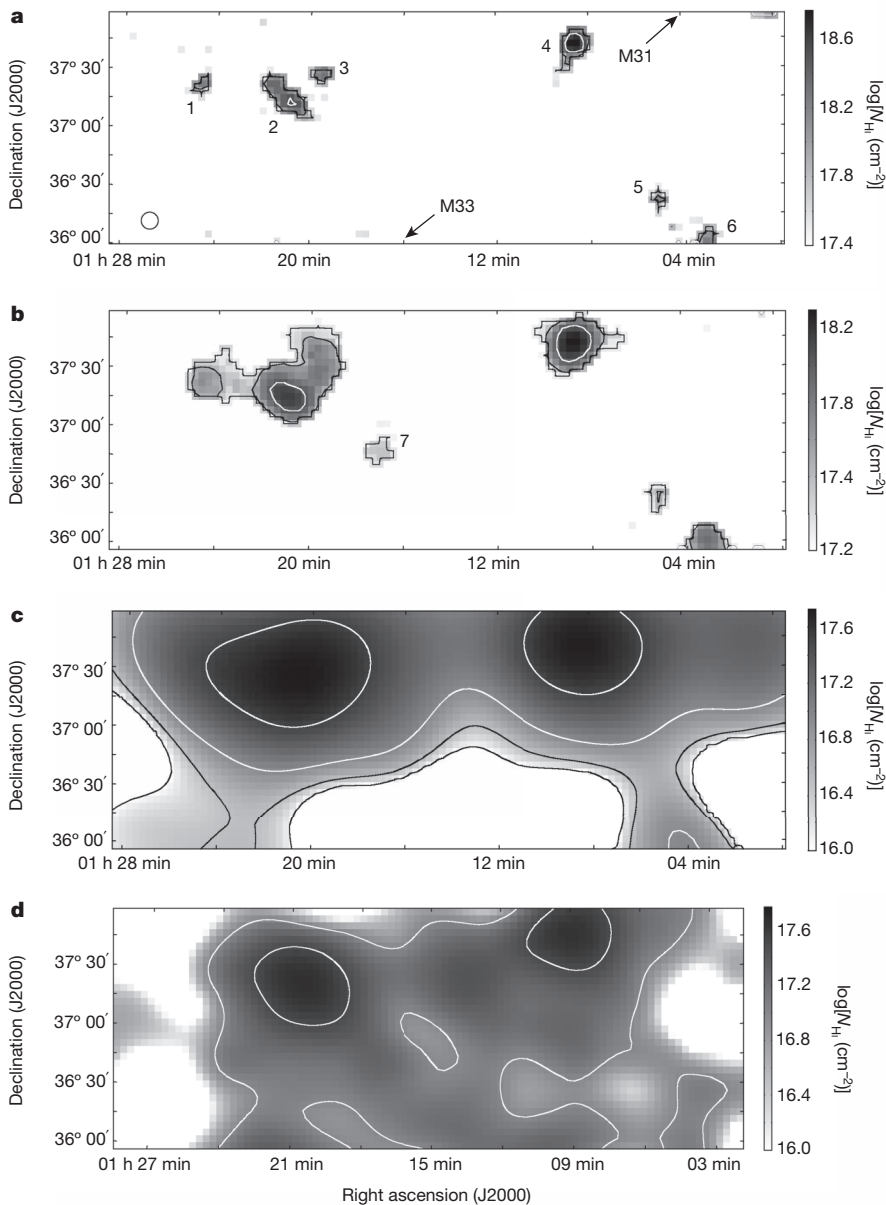


Figure 1 | H I column density maps. Maps of 21-cm emission over a 12 square-degree region between M31 and M33^{18,19}. The data from which these plots were compiled are available in Supplementary Information. **a**, Column density map of H I (in units of cm^{-2}) of the section of the area between M31 and M33 mapped with the GBT. This is a result of nearly 250 h of integration. The 3σ sensitivity limit in N_{HI} is $2.7 \times 10^{17} \text{ cm}^{-2}$ for a linewidth of 25 km s^{-1} at $9'$ angular resolution with a velocity resolution of 5 km s^{-1} . The contours are for $\log(N_{\text{HI}}) = 17.5, 18.0, 18.5$. There are six confirmed H I clouds, labelled in order of decreasing right ascension. M31 is to the northwest and M33 to the southeast, as indicated by the arrows. Both galaxies are about five degrees from the respective edges of the map. **b**, The GBT data, smoothed to a $15'$ resolution to match the sensitivity of the WSRT data ($1 \times 10^{17} \text{ cm}^{-2}$). A seventh cloud is now visible, labelled 7. The contours are for $\log(N_{\text{HI}}) = 17.0, 17.5, 18.0$. **c**, The GBT data, smoothed to a $49'$ resolution to match the angular resolution of the WSRT data. The contours are for $\log(N_{\text{HI}}) = 16.0, 16.5, 17.0, 17.5$. **d**, Part of the WSRT H I survey³ that first detected neutral gas between M31 and M33, at an angular resolution of $49'$ and a velocity resolution of 18 km s^{-1} . H I emission was detected over a wide area at $N_{\text{HI}} \geq 10^{17} \text{ cm}^{-2}$, most of it only 2–3 times the noise level. The contours are for $\log(N_{\text{HI}}) = 17.0, 17.5$.

is two to three orders of magnitude larger than its H I mass. The presence of an ionized component, however, would decrease the amount of dark matter necessary to match the virial mass. The free-fall time for these clouds, or the time it would take for these clouds to freely collapse under their own gravity, is $\sim 400 \text{ Myr}$ and the crossing time, the time it would take for a parcel of gas to cross the length of the cloud, is $\sim 100 \text{ Myr}$. These times are quite short to have resulted from the interaction between M31 and M33 proposed to have occurred a few billion years ago^{5,10} unless confined by an external pressure. The warm-hot intergalactic medium (WHIM)⁴ at a temperature $\sim 10^6 \text{ K}$ and of density $\geq 10^{-7} \text{ cm}^{-3}$ would supply the pressure if the clouds have a temperature of $\sim 10^4 \text{ K}$, consistent with the values inferred from the cloud linewidths. The WHIM densities needed are comparable to those predicted¹⁴ beyond the virialized region of galaxies, therefore these clouds could be in complete pressure equilibrium with the WHIM.

These clouds have several possible origins. First, they may be primordial, gas-rich objects similar to the dwarf spheroidal or dwarf irregular galaxies in the Local Group, but this does not explain why the gas seems to lie along a connecting structure, even when resolved into clouds. Second, the clouds may be gas that is accreting onto sub-haloes. This might occur naturally if the gas is part of a cosmic filament. If instead the gas is tidal in origin, it is likely to be moving at

relative speeds that exceed the escape velocities of sub-haloes, making accretion unlikely. Third, the clouds may be analogous to tidal dwarf galaxies¹⁵. This would account for their spatial and kinematical distribution with respect to M31 and M33. If so, the clouds would need to be in pressure equilibrium with the WHIM, so that they could persist for a few billion years following the interaction between M31 and M33. It is also possible that there may have been a more recent interaction that produced these clouds, such as M31 with IC10 or some other object. These clouds contain no evidence of stars, however, and do not fall on the Tully–Fisher relation, as one system of tidal dwarfs is known to do¹⁵. Last, the clouds could be transient objects condensing from an intergalactic filament, as originally proposed^{3,16}. This could explain their spatial distribution, as well as the lack of stellar overdensities. A recent simulation¹⁷ of a Milky Way sized galaxy has produced analogous material out to $\sim 100 \text{ kpc}$ with H I masses $\sim 10^5 M_{\odot}$, suggesting that the clouds are most probably condensations from an intergalactic filament.

We conclude that the H I clouds between M31 and M33 are a unique population, lacking a clear analogue in other members of the Local Group, such as the dwarf galaxies or HVCs. Although our current results suggest that the clouds may arise in an intergalactic filament, and thus are potential fuel for star formation in M31 and/or M33, the

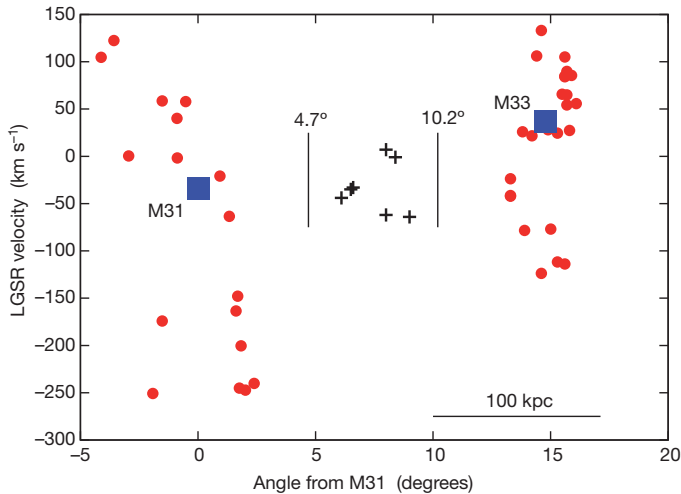


Figure 2 | A position-velocity plot of the H I clouds and selected Local Group objects. The local group standard of rest (LGSR) velocities were calculated using the NASA Extragalactic Database. Large blue squares indicate M31 and M33. Filled red circles are the high-velocity clouds (HVCs) of each galaxy^{20–23}. Crosses show clouds detected in the GBT maps; the vertical bars mark the GBT map boundaries, in terms of angle from M31. The HVCs lie within ~ 50 kpc of each galaxy, whereas the new clouds are found ~ 100 kpc from both galaxies. The new clouds also have an inter-cloud velocity dispersion of 25 km s^{-1} , compared to the $70\text{--}130 \text{ km s}^{-1}$ for the HVCs.

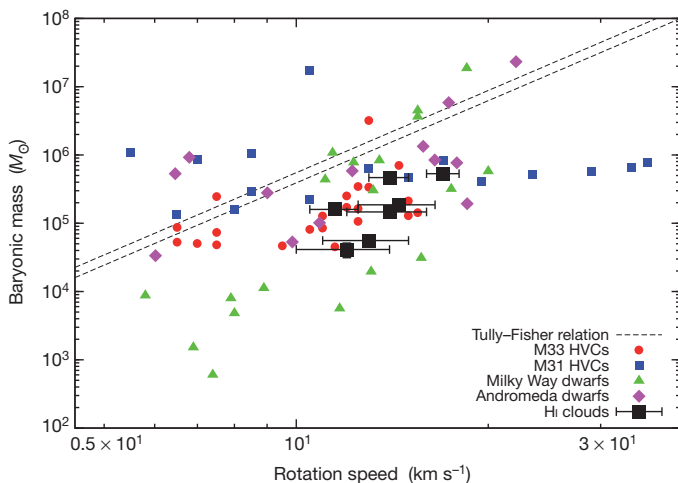


Figure 3 | A plot of baryonic mass versus the equivalent circular rotation speed. This figure compares the newly detected H I clouds (black filled squares with 1σ error bars), the HVCs of M31 and M33 (squares, circles), Milky Way dwarf satellite galaxies²⁴ (triangles) and the Andromeda dwarfs²⁵ (diamonds) to the baryonic Tully-Fisher relation²⁶ with $\pm 1\sigma$ uncertainty (dashed lines). We assume that all of the mass is in the neutral atomic gas and that $M_{\text{baryonic}} = 1.33 \times M_{\text{HI}}$ to account for helium. The masses are plotted in units of solar masses. The presence of an ionized component will increase the baryonic mass and move the clouds closer to the relation, but we have no way at present to estimate its magnitude. The effective circular rotation speed is $v_{\text{rot}} = \text{FWHM}/2$ where FWHM is the full-width at half-maximum of the H I line. This assumption holds in the case where the gas may be in rotation or is a turbulently supported, spherical system with an assumed harmonic radius of $R/2$, where R is the cloud radius, measured to the same column density contour as the diameter in Table 1. The scatter in mass-rotation velocity is 0.5 dex for the clouds, 0.8 dex for the Andromeda dwarfs and M33's HVCs, 1.2 dex for M31's HVCs, and 1.8 dex for the Milky Way dwarfs. The average errors (in dex) for the rotation velocities $\langle \sigma_v \rangle$ and masses $\langle \sigma_M \rangle$ are respectively 0.05 and 0.1 for M33's HVCs, 0.05 and 0.06 for M31's HVCs, 0.1 and 0.2 for the Milky Way dwarfs, 0.1 and 0.7 for the Andromeda dwarfs and 0.06 and 0.08 for the H I clouds.

question of their origin needs further consideration. The new clouds we report here were discovered in only about half of our survey time and thus are not at the full sensitivity that we intend to achieve. The region we have studied is only a fraction of the area around M31 reported³ to have diffuse H I, so the clouds measured here may be the first representatives of a much larger population.

Received 13 December 2012; accepted 18 March 2013.

1. Leroy, A. K. *et al.* The star formation efficiency in nearby galaxies: measuring where gas forms stars effectively. *Astron. J.* **136**, 2782–2845 (2008).
2. Shull, J. M., Smith, B. D. & Danforth, C. W. The baryon census in a multiphase intergalactic medium: 30% of the baryons may still be missing. *Astrophys. J.* **759**, 23–37 (2012).
3. Braun, R. & Thilker, D. A. The WSRT wide-field H I survey II. Local Group features. *Astron. Astrophys.* **417**, 421–435 (2004).
4. Davé, R. *et al.* Baryons in the warm-hot intergalactic medium. *Astrophys. J.* **552**, 473–483 (2001).
5. Bekki, K. Formation of a giant HI bridge between M31 and M33 from their tidal interaction. *Mon. Not. R. Astron. Soc.* **390**, L24–L28 (2008).
6. Lockman, F. J., Free, N. L. & Shields, J. C. The neutral hydrogen bridge between M31 and M33. *Astron. J.* **144**, 52–58 (2012).
7. Popping, A., Davé, R., Braun, R. & Oppenheimer, B. D. The simulated H I sky at low redshift. *Astron. Astrophys.* **504**, 15–32 (2009).
8. Maloney, P. Sharp edges to neutral hydrogen disks in galaxies and the extragalactic radiation field. *Astrophys. J.* **414**, 41–56 (1993).
9. Ibata, R. *et al.* The haunted halos of Andromeda and Triangulum: a panorama of galaxy formation in action. *Astrophys. J.* **671**, 1591–1623 (2007).
10. McConnachie, A. W. *et al.* The remnants of galaxy formation from a panoramic survey of the region around M31. *Nature* **461**, 66–69 (2009).
11. Lewis, G. F. *et al.* PAndAS in the mist: the stellar and gaseous mass within the halos of M31 and M33. *Astrophys. J.* **763**, 4–13 (2013).
12. Tully, R. B. & Fisher, J. R. A new method of determining distances to galaxies. *Astron. Astrophys.* **54**, 661–673 (1977).
13. McGaugh, S. S., Schombert, J. M., Bothun, G. D. & de Blok, W. J. G. The baryonic Tully-Fisher relation. *Astrophys. J.* **533**, L99–L102 (2000).
14. Fukugita, M. & Peebles, P. J. E. The cosmic energy inventory. *Astrophys. J.* **616**, 643–668 (2004).
15. Gentile, G. *et al.* Tidal dwarf galaxies as a test of fundamental physics. *Astron. Astrophys.* **472**, L25–L28 (2007).
16. Maller, A. H. & Bullock, J. S. Multiphase galaxy formation: high-velocity clouds and the missing baryon problem. *Mon. Not. R. Astron. Soc.* **355**, 694–712 (2004).
17. Fernández, X., Joung, M. R. & Putman, M. E. The origin and distribution of cold gas in the halo of a Milky-Way-mass galaxy. *Astrophys. J.* **749**, 181–192 (2012).
18. Chynoweth, K. *et al.* Neutral hydrogen clouds in the M81/M82 group. *Astron. J.* **135**, 1983–1992 (2008).
19. Boothroyd, A. I. *et al.* Accurate galactic 21-cm H I measurements with the NRAO Green Bank Telescope. *Astron. Astrophys.* **536**, A81 (2011).
20. Thilker, D. A. *et al.* On the continuing formation of the Andromeda galaxy: detection of H I clouds in the M31 halo. *Astrophys. J.* **601**, L39–L42 (2004).
21. Grossi, M. *et al.* H I clouds in the proximity of M33. *Astron. Astrophys.* **487**, 161–175 (2008).
22. Westmeier, T., Brüns, C. & Kerp, J. Relics of structure formation: extra-planar gas and high velocity clouds around the Andromeda Galaxy. *Mon. Not. R. Astron. Soc.* **390**, 1691–1709 (2008).
23. Putman, M. E. *et al.* The disruption and fueling of M33. *Astrophys. J.* **703**, 1486–1501 (2009).
24. McGaugh, S. S. & Wolf, J. Local Group dwarf spheroidals: correlated deviations from the baryonic Tully-Fisher relation. *Astrophys. J.* **722**, 248–261 (2010).
25. Tollerud, E. J. The SPLASH survey: spectroscopy of 15 M31 dwarf spheroidal satellite galaxies. *Astrophys. J.* **752**, 45–73 (2012).
26. McGaugh, S. S. The baryonic Tully-Fisher relation of gas-rich galaxies as a test of Λ CDM and MOND. *Astron. J.* **143**, 40–54 (2012).

Supplementary Information is available in the online version of the paper.

Acknowledgements D.J.P. is an Adjunct Assistant Astronomer at the National Radio Astronomy Observatory; F.J.L. is an Adjunct Professor in the Department of Physics, West Virginia University. S.A.W. acknowledges the student observing support (GSSP11-012) provided by the NRAO for this project. The NRAO is a facility of the NSF operated under cooperative agreement by Associated Universities, Inc. D.J.P. acknowledges support from NSF CAREER grant AST-1149491. S.S.M. acknowledges support in part by NSF grant AST-0908370.

Author Contributions All authors assisted in the development and writing of this work. S.A.W. is the Principal Investigator, and was responsible for data collection, processing and analysis. D.J.P. and F.J.L. assisted in the experimental design, data collection and analysis. S.S.M. provided the techniques of estimating the baryonic masses. E.J.S. provided necessary insights on potential interactions with M31 and ways of estimating circular rotation speeds. All authors aided in the interpretation of the results and provided comments for revisions to this work.

Author Information Reprints and permissions information is available at www.nature.com/reprints. The authors declare no competing financial interests. Readers are welcome to comment on the online version of the paper. Correspondence and requests for materials should be addressed to S.A.W. (swolfe4@mix.wvu.edu).